



HAL
open science

A simplified prediction of contact forces for tire-road noise modeling: theoretical and experimental approach

Fabienne Anfosso-Lédée, Julien Cesbron, Honoré P. Yin, Denis Duhamel,
Donatien Le Houedec

► **To cite this version:**

Fabienne Anfosso-Lédée, Julien Cesbron, Honoré P. Yin, Denis Duhamel, Donatien Le Houedec. A simplified prediction of contact forces for tire-road noise modeling: theoretical and experimental approach. INTERNOISE 2007, 2007, Istanbul, Turkey. pp.1-9. hal-01007803

HAL Id: hal-01007803

<https://hal.science/hal-01007803v1>

Submitted on 2 Sep 2024

HAL is a multi-disciplinary open access archive for the deposit and dissemination of scientific research documents, whether they are published or not. The documents may come from teaching and research institutions in France or abroad, or from public or private research centers.

L'archive ouverte pluridisciplinaire **HAL**, est destinée au dépôt et à la diffusion de documents scientifiques de niveau recherche, publiés ou non, émanant des établissements d'enseignement et de recherche français ou étrangers, des laboratoires publics ou privés.



Distributed under a Creative Commons Attribution 4.0 International License



INTER-NOISE 2007

28-31 AUGUST 2007

ISTANBUL, TURKEY

A simplified prediction of contact forces for tire-road noise modeling: theoretical and experimental approach.

Fabienne Anfosso-Lédée^a, Julien Cesbron^b

Laboratoire Central des Ponts et Chaussées

Centre de Nantes

BP 4129

44 341 Bouguenais cedex

FRANCE

Honoré Yin^c, Denis Duhamel^d

Ecole Nationale des Ponts et Chaussées

LAMI

77 455 Marne la Vallée cedex 2

FRANCE

Donatien Le Houédec^e

Ecole Centrale de Nantes

GeM

44 321 Nantes cedex 3

FRANCE

ABSTRACT

The modeling of dynamic contact forces between a tire tread and a road surface is an essential input for the prediction of absolute tire/road noise levels.

Here, an original approach called the Two-scale Iterative Method (TIM) is presented for the analytical prediction of the contact force distribution between a rough road surface and a tire. It is based on an approximate relation between the normal contact force and the relative displacement at the tip of each punch, on which a contact law is known analytically or calculated numerically. The relation takes into account the interacting effect between the punches. Then pressure distribution on each individual punch can be calculated by traditional numerical methods at a local scale. The calculation is much faster than other existing methods, and real 3D contact patches with a large number of asperities can be calculated.

An experimental validation is performed using a digital pressure sensing device (Tekscan©). Static contact pressure distributions are measured and simulated for a slick tire on eight different road surfaces. A fair agreement is obtained between measurements and calculation of contact area, mean pressure and pressure distribution in the contact patch. Thus, the use of this model for tire-road noise modeling is very encouraging.

^a Email address: fabienne.anfosso@lcpc.fr

^b Email address: julien.cesbron@lcpc.fr

^c Email address: yin@lami.enpc.fr

^d Email address: duhamel@lami.enpc.fr

^e Email address: donatien.lehouedec@ec-nantes.fr

1 INTRODUCTION

The modeling of dynamic contact forces between a tire tread and a road surface is an essential input for the prediction of absolute tire/road noise levels. In this problem, the contact pressure at the interface between a rigid surface and a rubber half-space must be calculated. The classical approach is based on the derivation of an influence matrix that links the displacement at points on the surface to the pressure in the contact area. The problem is solved by an iterative inversion process until the equilibrium of pressures is achieved. This is described by Johnson [1] and will be referenced in this paper as a Matrix Inversion Method (MIM). This method has been widely used, especially in the context of tire-road noise by Wullens and Kropp [2], Klein et al. [3]. Its efficiency is limited to a reasonable number of punches. In this paper, a more efficient approach is proposed, leading to a simplified calculation scheme that makes possible the prediction of contact forces on larger areas or with a larger amount of asperities. It is called the Two-scale Iterative Method (TIM) as the pressure distribution in the contact area is calculated at two iterative scales. At macro-scale, the force on each punch is calculated from a local load-penetration approximation, and at micro-scale, the pressure distribution on each punch is calculated using a local MIM approach. The resulting calculation is time-efficient, even when the number of punches is large as in the case of tire-road contact.

In the first part, the method is presented and examples of tire-road contact patches are given at a fine pressure scale. Then an experimental validation is performed using a digital pressure sensing device (Tekscan©). Correlations between measured and calculated pressures are discussed.

2 THE MODELING APPROACH BY TWO-SCALE ITERATIVE METHOD (TIM)

2.1 General hypothesis

The tire tread is modeled by a perfectly flat three-dimensional elastic half-space with a Young's modulus E and a Poisson's ratio ν . The road surface is described by N perfectly rigid indenters with random shapes. The surfaces in contact are frictionless, which means that there is no tangential tractions and only the normal pressure is taken into account in the contact area. The contact problem is solved in statics along the driving path line for each space step Δx . The time-dependence of the contact forces can be obtained by a combination of the static results at each time step $\Delta t = \Delta x/V$, where V is the car velocity.

2.2 Macro-scale: calculation of contact forces at each tip

In many cases, the solution for single rigid punch acting on an elastic half-space can be described by an analytical relation between the total load on the punch P and the total depth of penetration at the tip of the punch δ . This is called the load-penetration function and can also be determined by numerical methods if the analytical solution is not available. These relations take the form:

$$P = C E^* \delta^\gamma \quad (1)$$

where C is a constant depending on the geometry and the size of the punch, γ is also a constant depending on the shape of the punch, and $E^* = E/(1-\nu^2)$. For instance for a spherical punch of radius R , the Hertz's theory gives $C = \frac{4}{3}\sqrt{R}$ and $\delta = \frac{3}{2}$.

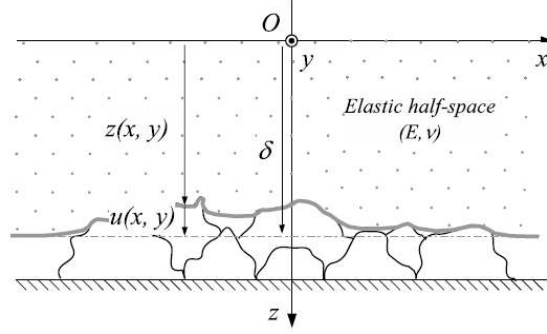


Figure 1: Contact between an elastic half-space and several rigid punches.

In the case of a surface with many punches (Figure 1), the normal contact force P_k on the k^{th} punch can be expressed for a global penetration δ :

$$P_k = C_k E^* [(\delta - z_k - u_k)H(\delta - z_k - u_k)]^{1/2} \quad (2)$$

where H is the Heaviside's function and u_k is the normal displacement of the elastic half-space at the tip of the k^{th} punch due to the other punches. This displacement can be expressed using the Boussinesq's approximation:

$$u_k = \sum_{\substack{l=1 \\ l \neq k}}^N T_{kl} P_l \quad \text{with} \quad T_{kl} = \frac{1}{\pi E^* \sqrt{(x_k - x_l)^2 + (y_k - y_l)^2}} \quad (3)$$

The combination of the last two equations leads to the resolution of a system of non linear equations with unknowns P_k that can be solved with the Newton-Raphson's iterative scheme.

2.3 Micro-scale: calculation of pressure distribution

In some applications, the determination of the contact force P_k at the tip of each punch can be sufficient. However, it is also possible to calculate the pressure distribution on the contact surface by using a local MIM (noted LMIM) at the scale of an individual punch. The interface is discretized into square identical elements on which the pressure is assumed constant. The pressure distribution \mathbf{p}^0 is calculated from the forces P_k obtained at macro-scale. The pressure vector is written:

$$\mathbf{p}^0 = \{\mathbf{p}_1^0, \dots, \mathbf{p}_k^0, \dots, \mathbf{p}_N^0\} \quad (4)$$

The sub-vector \mathbf{p}_k^0 corresponding to the pressure distribution on the k^{th} punch is calculated by LMIM for a known loading force P_k :

$$\begin{bmatrix} C_{k_{11}} & \cdots & C_{k_{1n_k}} & -1 \\ \vdots & \ddots & \vdots & \vdots \\ C_{k_{n_k 1}} & \cdots & C_{k_{n_k n_k}} & -1 \\ 1 & \cdots & 1 & 0 \end{bmatrix} \begin{Bmatrix} p_{k_1}^0 \\ \vdots \\ p_{k_{n_k}}^0 \\ \delta_k \end{Bmatrix} = \begin{Bmatrix} -z_{k_1} \\ \vdots \\ -z_{k_{n_k}} \\ P_k \end{Bmatrix} \quad (5)$$

where δ_k the local penetration and n_k the number of elements on punch k . $C_{k_{ij}}$ is the influence coefficient between element i and element j . In a first approximation, this vector \mathbf{p}^0 gives a good prediction of the pressure distribution in the contact zone. It can be improved by the introduction of an iterative process that will not be described here but can be found in [5].

2.4 Calculation of tire-road print contact area

The TIM approach was successfully compared with other numerical methods (MIM, FEM) on small surfaces with spherical and flat-ended punches [5]. The convergence of the iterative scheme of the TIM is faster than the classical MIM by a factor of more than 10. This ratio is even higher when the number of punches increases (a factor of 70 was observed in the case of 24 punches). This makes the TIM an adapted tool for the prediction of contact forces between a tire and a rough road surface including a large amount of punches. To demonstrate the capacity of the method, calculations were performed at the scale of a real tire print on a road surface. The modeling principle is summarized in Figure 2.

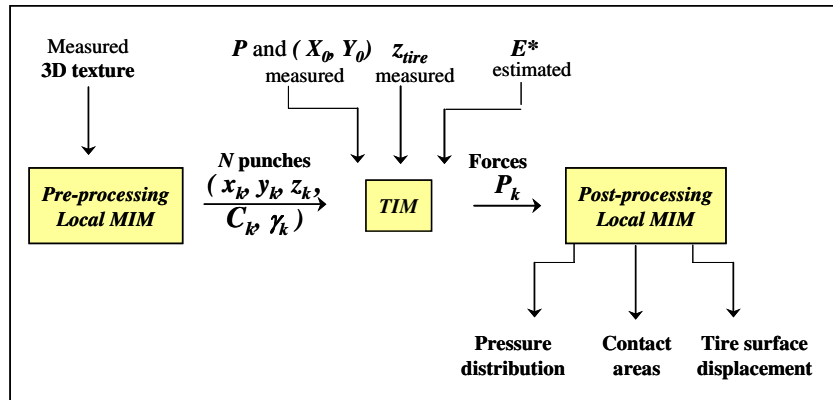


Figure 2: Modeling principle of static tire-road contact.

First, the 3D texture of the surface is measured by an optical device. An array of 955000 coordinates distributed on a 200 mm by 191 mm rectangular surface with a spacing of 0.2 mm gives the geometrical description of the surface. This data set is then pre-processed by a labeling procedure that identifies and numbers the punches. This procedure is based on an algorithm used in image processing for picture segmentation and shape identification. Then, for each identified punch, the load-penetration law is determined by a numerical approach, using a local MIM. Additional input parameters for the model such as the total load P applied on the wheel, or the Young's modulus E of the tire material can be measured or estimated. For a better accuracy of the model, it is also possible to introduce the curved geometry of the tire, and the position (X_0, Y_0) of the point where the total load P is applied.

Then the TIM is applied to give the force distribution on all the defined punches. Finally, in order to get the pressure distribution, the LMIM is applied locally on each punch.

An example of the calculation result in terms of pressure distribution is shown in Figure 3 for two different surfaces. One is a model surface with spherical punches of 8, 10 and 12 mm diameter and randomly distributed. The second one is a real Dense Asphalt Concrete road surface with aggregate size of maximum 10 mm. A total load of 2950 N is applied on the surfaces by a slick tire of diameter 57 cm and width 186 mm. The Young's modulus of the tire material is $E=2.4$ MPa. The first contact pattern was obtained in about 10 minutes and the second one in less than 1 hour on a standard computer.

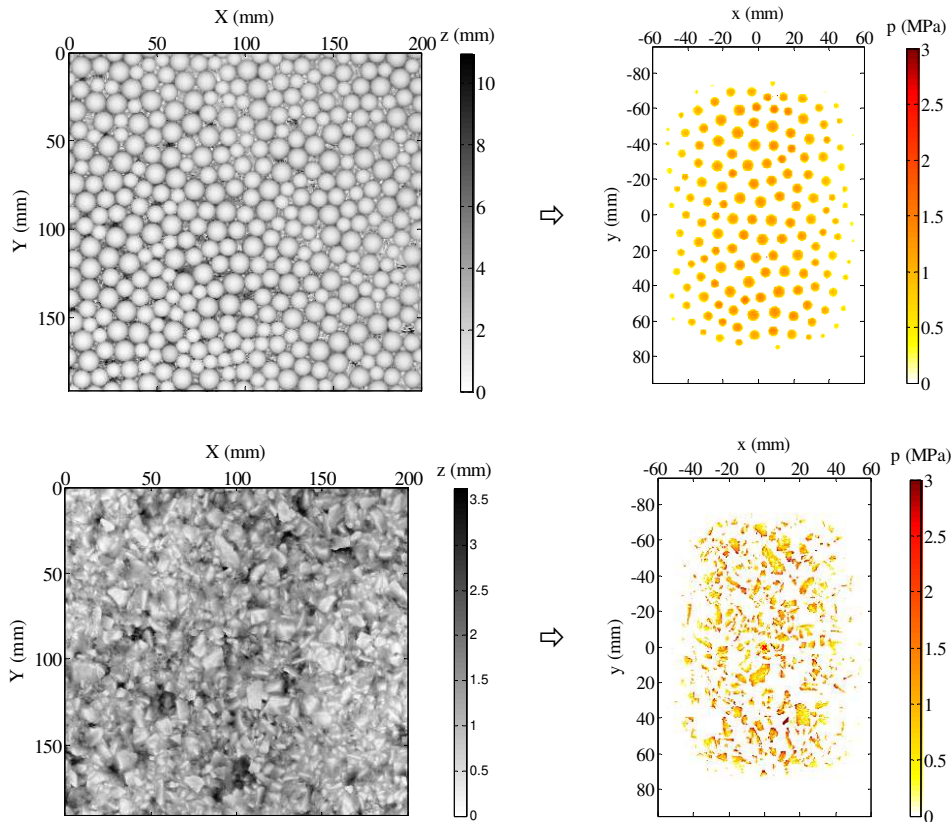


Figure 3: Pressure distribution on a model surface with spherical punches (top) and on a Dense Asphalt Concrete 0/10 (bottom). Measured 3-D texture (left) and calculated pressure distribution (right).

3 EXPERIMENTAL VALIDATION

3.1 Pressure measuring device

For the validation of the TIM model, a digital pressure sensing device developed by Tekscan© was used. The system is composed of a matrix-based sensor linked to an acquisition card and a P.C. (Figure 4). The data acquisition display and analysis is monitored by software. The contact pressure distribution between two bodies can be measured in real time, at a frequency step of 207 Hz. The sensor consists of two thin, flexible polyester sheets which have electrically conductive electrodes placed in a regular mesh. Between the sheets, a semi-conductive layer provides an electrical resistance that varies proportionally to the pressure applied. Thus, the sensor is an array of force sensitive cells measuring the pressure distribution between the two surfaces. The sensor used in the experiment (ref 3150) has an active area of 432 mm x 368 mm divided in an array of 2288 square cells of side $\Delta x = 8.38$ mm. It is very thin (0.1 mm thickness) which minimizes the intrusion when placed between the two contacting bodies.

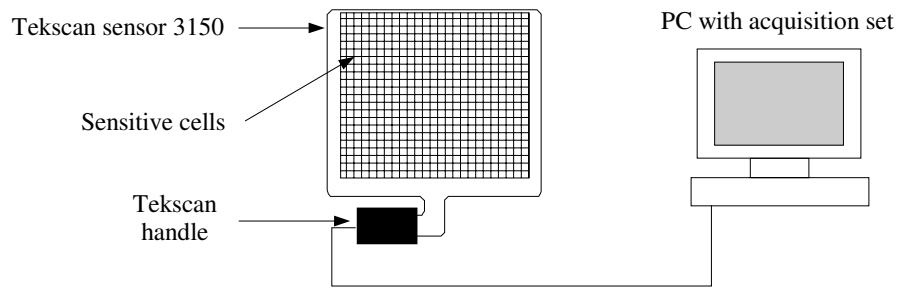


Figure 4: Measurement device.

However the measurement system provides raw data between 0 and 255, and a calibration must be applied in order to link these data with pressure or force values. The sensor response is not linear. It depends on the sensitivity of the sensor, on the geometry of the surfaces and on the loading procedure. It is recommended by the manufacturer to calibrate the sensor for a loading condition similar to the one in the measured case. In practice, the total load applied on the tire, measured independently on a weighting device, is used as the calibration reference on each measurement. It is assumed that the relation between the pressure and the digital values is linear, within the studied range.

3.2 Measurement procedure

In a first validation step, static measurements of contact pressure between a rubber block and small samples with spherical indenters were performed. The results lead to a very good agreement. They were presented in [4]. Here the static contact between a real tire and pavement samples is studied for eight different road surfaces.

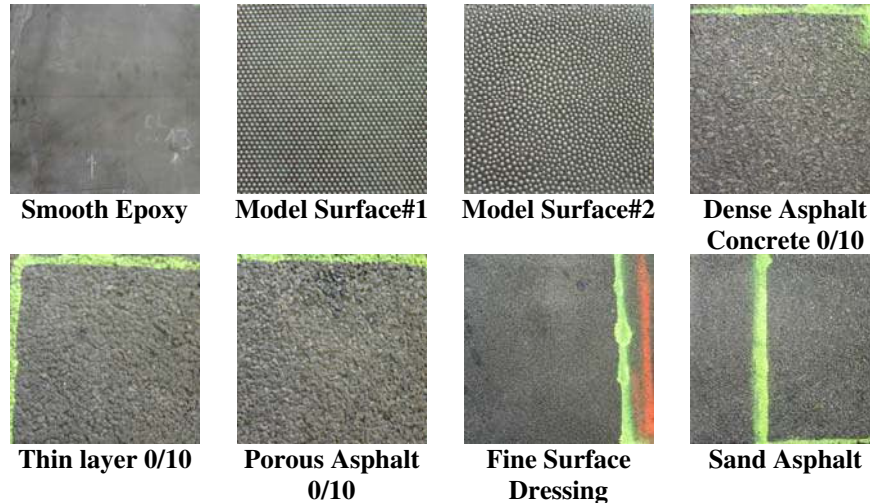


Figure 5: Description of the tested road surfaces.

The model surface #1 is made of spheres of radius 10 mm with a periodic honeycomb distribution. The model surface #2 is made of spheres of radius 8, 10 and 12 mm with a random distribution. The other five surfaces are taken from real roads. Three are asphalt concretes with 10 mm maximum aggregate size. The last two surfaces are surface dressing with small size protruding aggregates.

All surface samples are 0.4 m by 0.4 m. For all of them, texture measurements were performed as described previously.

The right rear wheel of a passenger car fitted with a slick tire is loaded on each surface sample. The tire load $P=2950$ N was measured previously. Each measurement is repeated four times.



Figure 6: Description of the contact experiment.

3.3 Measurement results and comparison with calculations

For the comparison between measurements and calculation, additional information and processing is needed. First, an equivalent Young's modulus of the tire material was estimated so that the calculated mean contact pressure is equal to the measured one on the smooth surface. The resulting value is $E=2.4$ MPa. Second, the spatial resolution of the calculated results is very fine ($\Delta x=0.4$ mm), whereas it is much wider for the measurement results (spacing of the sensor cell, i.e. $\Delta x=8.38$ mm). Thus the calculated results must be integrated on surfaces equivalent to the sensor cells.

A comparison of measured and calculated pressure distribution is shown in figure 7 for the model surface#1, the Dense Asphalt Concrete and the Porous Asphalt Concrete. It can be seen that qualitatively the agreement between measured and calculated prints is good. The periodicity of the model surface leads to periodic results in both cases. On surfaces with random texture, the pressure distribution is irregular. On the porous surface, both experiment and calculation show more gaps in the pattern (cells with a zero pressure) and higher maximum pressure than on the dense asphalt surface. The predicted contact areas are similar to the measured ones.

The predicted and measured contact areas and mean pressures are compared for the seven surfaces in figure 8. Each symbol corresponds to a road surface. The regression line is plain, the one-to-one line is dashed. The coefficients of the regression line are indicated together with the coefficient of correlation. The agreement between predicted and measured data is correct, especially when considering the accuracy of the measuring device (specified as $\pm 10\%$). The predicted contact area is slightly underestimated in the case of porous asphalt and thin layer asphalt, leading to an overestimation of the mean pressure for these two surfaces. It corresponds to the two roughest surfaces.

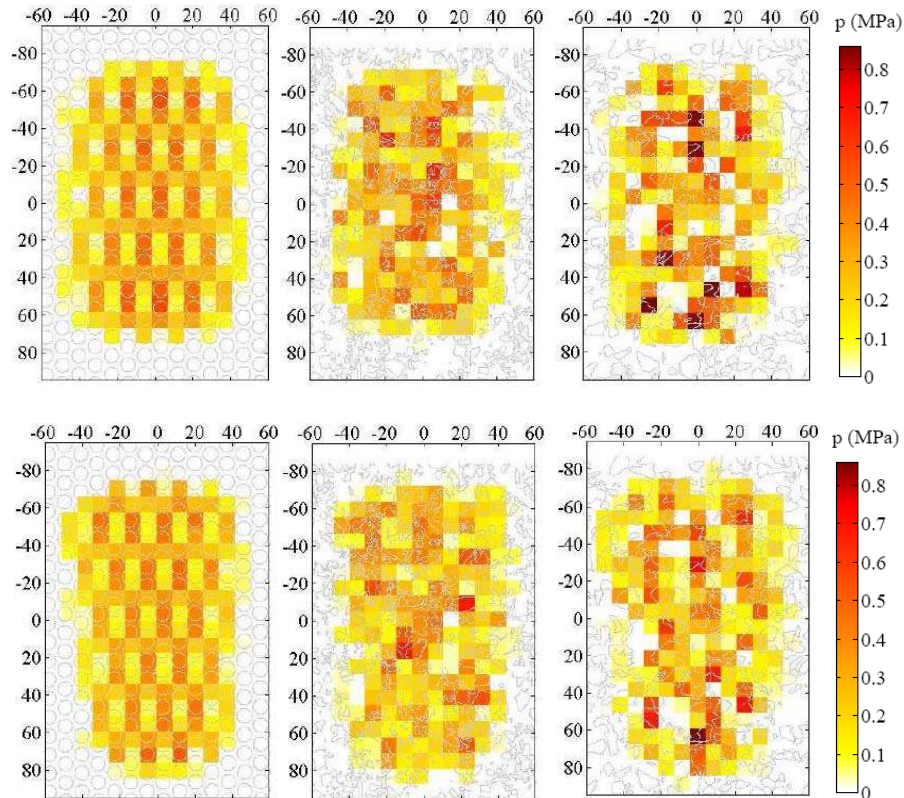


Figure 7: Calculated (top) and measured (bottom) tire/road pressure distributions for the Model Surface#1 (left), the Dense Asphalt Concrete (middle), and the Porous Asphalt (right)

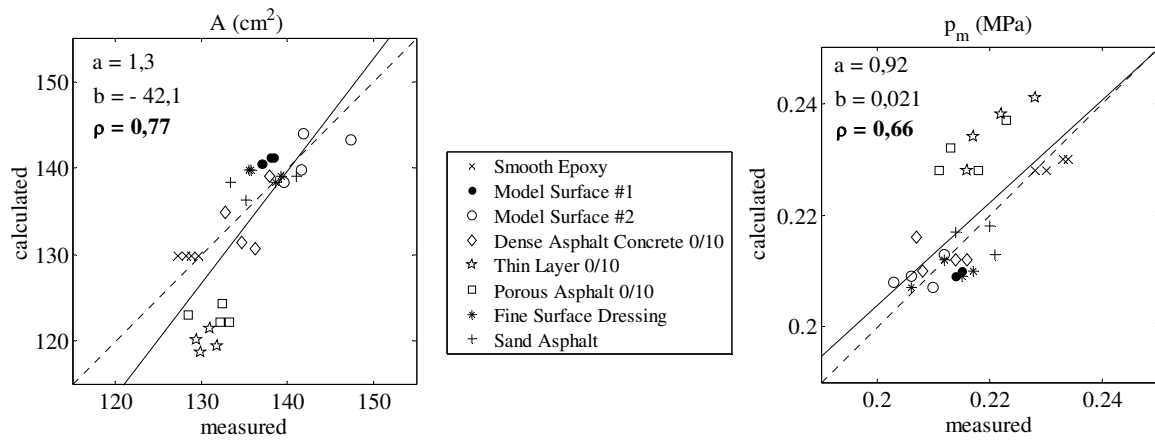


Figure 8: Comparison between calculated and measured contact areas (left) and mean pressure (right) for all surfaces.

Finally predicted pressure distributions are compared to measured ones, in each area corresponding to a sensor cell. The results for the model surface #1 with spherical punches, for the Dense Asphalt, and for the Porous Asphalt are displayed in Figure 9. Here again, the regression line is plain, with coefficients indicated at the top left, and the one-to-one line is dashed. The agreement is really encouraging, the slope of the regression line is close to one, and the regression coefficients are above 0.77. Comparisons for other surfaces are of the same order, except a slight overestimation of predicted results in the case of the last two surfaces at high pressure. These two surfaces (Fine Surface Dressing and Sand Asphalt) correspond to relatively smooth surfaces with very small (< 1.5 mm) protruding aggregates. The differences observed can be attributed to small spatial shifts between the experimental and the modeled mesh. In general for high pressure, the predicted results may be slightly

overestimated. This can be explained by the overload of the sensor for local pressures higher than 0.86 MPa. Furthermore, the approximation in the calculation of the pressure vector \mathbf{p}^0 at the local scale may be inaccurate when several adjacent punches are seen by the penetrating tire as one single punch.

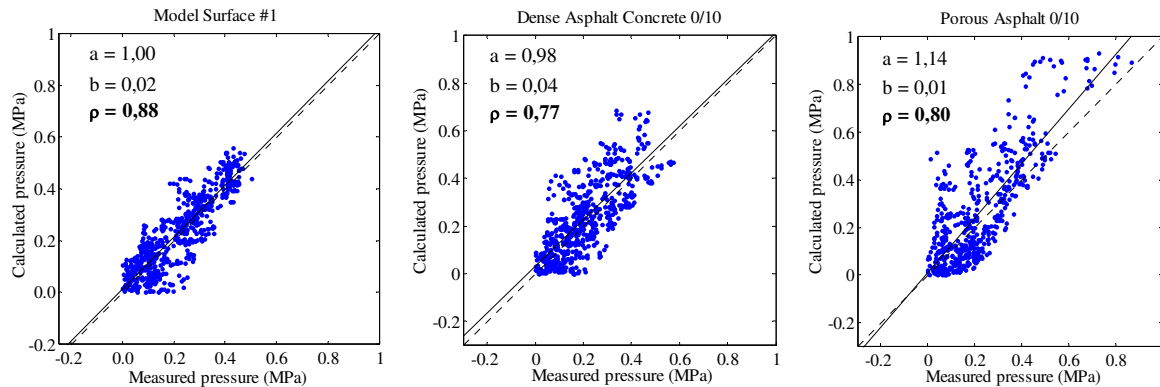


Figure 9: Comparison between calculated and measured pressure distributions in each sensor cell, for the Model Surface#1 (left), the Dense Asphalt Concrete (middle), and the Porous Asphalt (right)

4 CONCLUSIONS

In this paper, an efficient predicting approach for the modeling of contact stresses between a tire and a rough surface was presented and implemented. This method called TIM is much faster than other traditional methods, and makes possible the prediction of contact forces and pressures distributions on a surface with a large amount of punches. An experimental validation was performed by measuring contact pressure distribution in statics between the slick tire of a vehicle and different samples of road surfaces. The comparison between measurements and calculation is encouraging. Future works will address the dynamic measurements of tire-road contact, and the relations with the rolling noise emitted on different road textures.

5 ACKNOWLEDGEMENTS

The authors acknowledge the French-German cooperative program “DEUFRAKO” for the support of this research in the frame of the “P2RN” project.

6 REFERENCES

- [1] K.L. Johnson, *Contact mechanics*, Cambridge University Press (1985).
- [2] F. Wullens, W. Kropp, “A three-dimensional contact model for tyre/road interaction in rolling conditions”. *Acta Acustica united with Acustica* **90**, 702-711 (2004).
- [3] P. Klein, J-F. Hamet et F. Anfosso-Lédée, “An envelopment procedure for tire/road contact”. *Proceedings of SURF 2004, 5th Symposium on Pavement Surface Characteristics Roads and Airports*, World Road Association PIARC, Toronto (2004).
- [4] J. Cesbron, F. Anfosso-Lédée, D. Duhamel, H. Yin, and D. Le Houédec, “Prediction of contact stresses for tyre-road noise modelling”, *Proceedings of EURONOISE 2006*, paper SS26_50 (2006).
- [5] J. Cesbron, “Influence de la texture de chaussée sur le bruit de contact pneumatique-chaussée”, PhD thesis draft report, may 2007 (2007).